Cherenkov Detector Prototype for ILC Polarimetry

Daniela Käfer

Deutsches Elektronen Synchrotron (DESY), Notkestr. 85, 22607 Hamburg, Germany

E-mail: daniela.kaefer@desy.de

Abstract. Precise knowledge of all beam parameters is crucial to fully exploit the physics potential of the International Linear Collider (ILC). A sufficiently accurate measurement of the beam polarisation can only be achieved using dedicated high energy Compton polarimeters combined with well-designed Cherenkov detectors. The requirements have been evaluated and a suitable Cherenkov detector prototype has been designed, simulated and constructed accordingly. This prototype allows nearly all aspects of the final detector to be studied and has been operated successfully in a testbeam of which first results are presented as well.

1. High energy polarimetry at the ILC

The physics programme of the ILC will rely heavily on how accurately the relevant beam parameters can be controled [1, 2]. For electroweak processes, the absolute normalisation of events rates depends on luminosity and polarisation. The luminosity will be measured to a precision of 10^{-3} to 10^{-4}, while for the polarisation average an accuracy of 10^{-3} seems achievable. Contrary to luminosity and beam energy measurements for which permille level precisions have already been achieved, polarimetry needs to be improved by at least a factor of two.

Measurements of two dedicated polarimeters located up- and downstream of the e^+e^- interaction point will be combined with data from the e^+e^- annihilations themselves to determine the polarisation average. While the annihilation data will yield an absolute scale, the polarimeters provide fast measurements allowing to track variations over time (machine feedback) and to detect possible correlations with the luminosity or the polarisation of the other beam. Therefore, each polarimeter has to reach a systematic accuracy of at least $\delta\mathcal{P}/\mathcal{P} = 0.25\%$, further reducing systematic uncertainties and adding redundancy to the system. Two polarimeters per beam are required in order to measure the polarisation of the beams in collisions. Both polarimeters have been designed for operation at beam energies between 45 GeV and 500 GeV. A detailed description of the polarimeters can be found in [3].

Compton polarimetry ensures a non-destructive measurement of the longitudinal beam polarisation. Circularly polarised laser light is shot under a small angle onto the individual bunches causing typically $\mathcal{O}(10^3)$ electrons per bunch to undergo Compton scattering. The energy spectrum of the scattered particles depends on the product of laser and beam polarisations, so that the measured rate asymmetry w.r.t. the laser helicity is directly proportional to the beam polarisation. The differential Compton cross section vs. scattered electron energy exhibits a large polarisation asymmetry near the Compton edge energy, which hardly depends on the chosen beam energy [3]. Since the scattering angle in the laboratory frame is below 10 μrad, a magnetic chicane transforms the energy spectrum into a spatial distribution which is then measured by an array of Cherenkov detectors chosen for several reasons:

(i) It allows to measure the energy spectrum of many electrons arriving simultaneously.

(ii) Cherenkov radiation is independent of the electron energy ($\beta \approx 1$). The number of Cherenkov photons is directly proportional to the number of Compton electrons per channel.

(iii) Typical Cherenkov media are sufficiently rad-hard to withstand a high electron flux

The final detector will consist of staggered U-shaped aluminium channels lining the tapered exit window of the beam pipe as illustrated in figure 1(a). All channels are filled with a Cherenkov gas and read out by photodetectors. Compton-scattered electrons traversing the U-base emit Cherenkov photons reflected upward to the photodetectors.

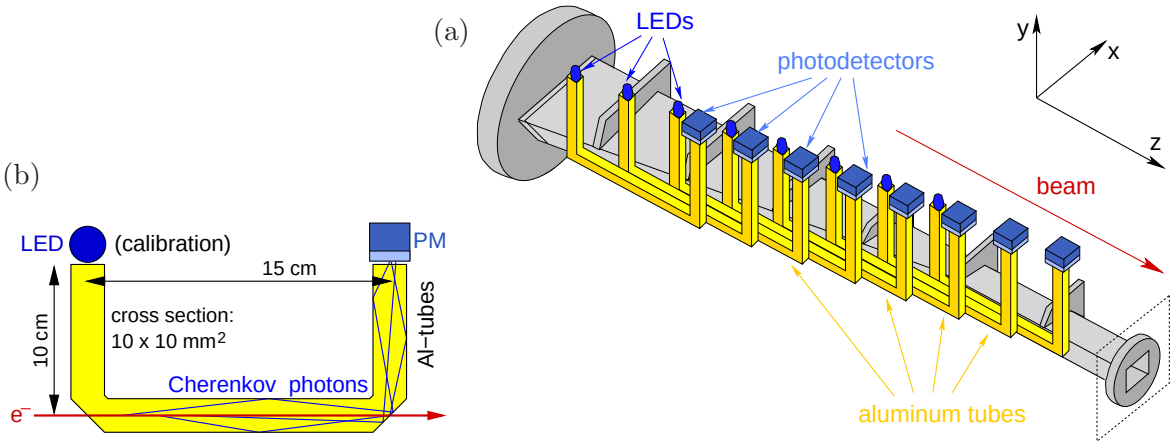

Figure 1: *(a) Illustration of a segmented Cherenkov detector; for better visibility with 8 instead of the forseen 20 readout channels. (b) Sketch of one gas-filled aluminium channel.*

2. Prototyp design and optical simulation

The design of the ILC polarimeter Cherenkov detectors is driven by a set of requirements, also used as a basis for the design, simulation and construction of a compact two-channel prototype:

- high & homogeneous light yield per Compton electron (geometry; smooth/planar surfaces; need high reflectivity also for short wavelengths due to the typical $1/\lambda^2$ distribution)
- gas- and light-tightness (control linearity; stabilize response over macroscopic times)
- thin inter-channel walls (avoid loosing electrons; avoid electromagn. shower background)
- robustness w.r.t. backgrounds (high-threshold gas avoids low-energetic e^- background; good layout keeps photodetectors & calibration source outside the beam plane)
- calibration system (monitor response in-situ, indep. of beam; in-between bunch trains)

The last two requirements lead to the idea of U-shaped channels, see figure 1(b). The longer the U-base, the more Cherenkov light is produced, but the alignment becomes more difficult and any additional reflections decrease the light yield. Simulations suggest a length of 15 cm is a reasonable choice. Contrary to the ILC-design of staggered channels, the prototype consists of only two parallel, non-staggered channels, but still allows to study all relevant aspects of the full detector, as well as the entire experimental setup. The detailed optical simulation of the prototype, based on GEANT4 [4] serves to determine key figures such as the photon yield per electron, the average number of reflections and possible asymmetry effects due to the utilized materials or chosen geometry, especially the square channel cross section.

Figure 2 shows the internal structure with a single electron (red) passing from left to right through the U-base of one detector channel. It emits Cherenkov light (green), which is reflected

upward at the end of the U-base towards the photodetector. Cherenkov light produced outside the channel structure in the ambient gas cannot reach the photodetectors. The square channel cross section of 8.5×8.5 mm^2 matches the anode layout of two multi-anode photomultipliers (MAPMs), such that one quadrant covers one detector channel. These MAPMs [5] were chosen based on earlier stand-alone studies of different photodetector types [6, 7].

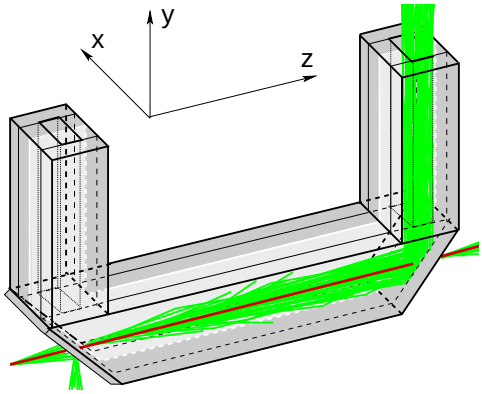

Figure 2: *Prototype simulation event display: An electron (red) passes from left to right through the U-base of one of the gas-filled aluminium channels emitting Cherenkov photons (green), which are reflected upward towards the photodetectors mounted on the hind U-leg. Both channels are separated by a thin foil (light grey). Due to a surrounding gas-filled box, Cherenkov radiation is also emitted before/after the electrons enter/exit the channels, but it cannot reach the photodetector.*

Two types of aluminium are implemented according to the reflectivities of different quality aluminium. Three of the four walls of each channel are made of diamond-milled aluminium with a reflectivity $R_{\text{diam}} \approx 80\%$, while the inter-channel wall consists of a 300 µm thin foil of rolled aluminium with only $R_{\text{roll}} \approx 36\%$. Perfluorobutane ($C_4F_{10}$) with its 10 MeV-threshold is chosen as Cherenkov gas making the detector robust against background from low energetic charged particles. Since a precise knowledge of the absolute photon yield is not crucial for the rate asymmetry measurement, the refractive index ($n = 1.0014$) is assumed independent of the wavelength, as well as of the temperature and pressure inside the detector box ($T = 20$ °C and $p = 1$ atm, respectively). Two scenarios with the same beam parameters (2D Gaussian profile, $\sigma_x = \sigma_y = 1.5$ mm) but different reflectivities for the inter-channel wall are simulated to study its influence on the expected light yield. While the distribution is symmetric about the x and z-axes when all four channel walls are simulated with the same reflectivity, a clear asymmetry emerges about the x-axis when the inter-channel wall is simulated with reduced reflectivity (figure 3).

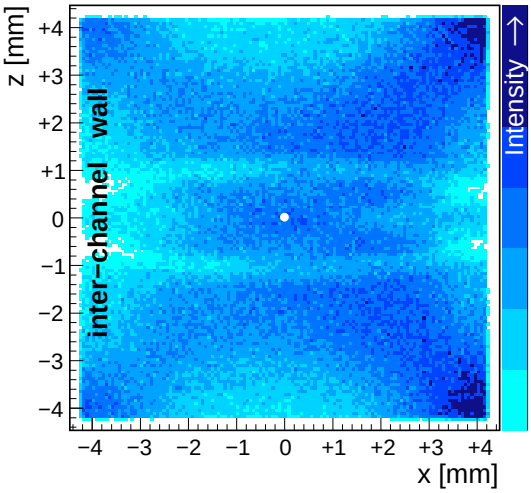

Figure 3: *Light yield at the photocathode for a reduced reflectivity of the inter-channel wall.*

This asymmetry, as well as the X-pattern (observed also for equal reflectivities of all walls) are due to a combination of the square channel cross section and the Cherenkov angle of perfluorobutane for relativistic electrons ($\Theta = 3°$). For central electrons, most photons are reflected once under a glancing angle. Photons emitted in the horizontal (vertical) plane illuminate the entire channel width at the photocathode, whereas (due to a larger effective channel cross section) photons emitted towards the corners illuminate only half the channel width on the same side of the reflecting wall. This explains the higher photon yield near the channel diagonals (X-pattern), and also the depletion on the side of the inter-channel wall due to its lower reflectivity. The reduced light yield visible in two narrow bands at $z = \pm 1$ mm stems from the 90° reflection at the end of the U-base.

Asymmetries in x and z are calculated for 4×4 beam positions (10^4 e^- each) of a grid scan. The beam y-position translates directly to the z-position in the photodetector readout plane (white dot in figure 3). The asymmetries are calculated as:

$$A_x = \frac{I_x^+ - I_x^-}{I_x^+ + I_x^-} \qquad \text{and} \qquad A_z = \frac{I_z^+ - I_z^-}{I_z^+ + I_z^-} \ ,$$

where I_x^+ (I_z^+) corresponds to the intensity in the right (upper) half of a channel and I_x^- (I_z^-) to the intensity in the left (lower) half, respectively. However, the asymmetries calculated for the simulated scans in the x and z directions are not displayed here, but are included in figure 6(a,b) on page 6 for comparison with the respective asymmetries calculated from testbeam data.

3. Beam tests at the ELSA accelerator

Beam tests with the prototype detector were performed in an external beam line at ELektronen-Stretcher-Anlage (ELSA). Its circumference of 164.4 m leads to a turn time of 548 ns for relativistic electrons [8]. During the testbeam period, electrons were injected into ELSA at an energy of 1.2 GeV and subsequently accelerated to 2.0 GeV. The beam is extracted for 4.0 s of every 5.1 s cycle, can be focussed to a spot size of about 1 mm to 2 mm, and the extracted current can be adjusted from about 10 pA to 200 pA by partial filling. This leads to respectively 35 to 700 electrons traversing the detector per ELSA turn, compared to about 250 electrons expected in the most populated channel of an ILC polarimeter Cherenkov detector.

The beam clock signal provides the gate for the QDC (charge sensitive ADC) and is adjusted to integrate over the filled part of a turn. The detector is filled with C_4F_{10} at 140 mbar and sits on its turnable base plate mounted on a movable stage. Moving the stage horizontally (x) and vertically (y) scans the incident beam position on the entrance window, so that the detector alignment w.r.t. the beam line can be obtained from beam data. The adjustment procedure requires one y-scan for each channel and a series of x-scans across both channels for different tilt angles α_y. Typically, for a tilted detector the maximal Cherenkov signal at a given beam position is smaller than for a perfectly aligned detector. Determining the beam x position of the highest signal for each tilt angle leads to $\alpha_y = (1.33 \pm 0.03)^\circ$ for the best alignment, which is approximated by $\alpha_y = 1.35^\circ$ due to the step size of the rotational mechanism.

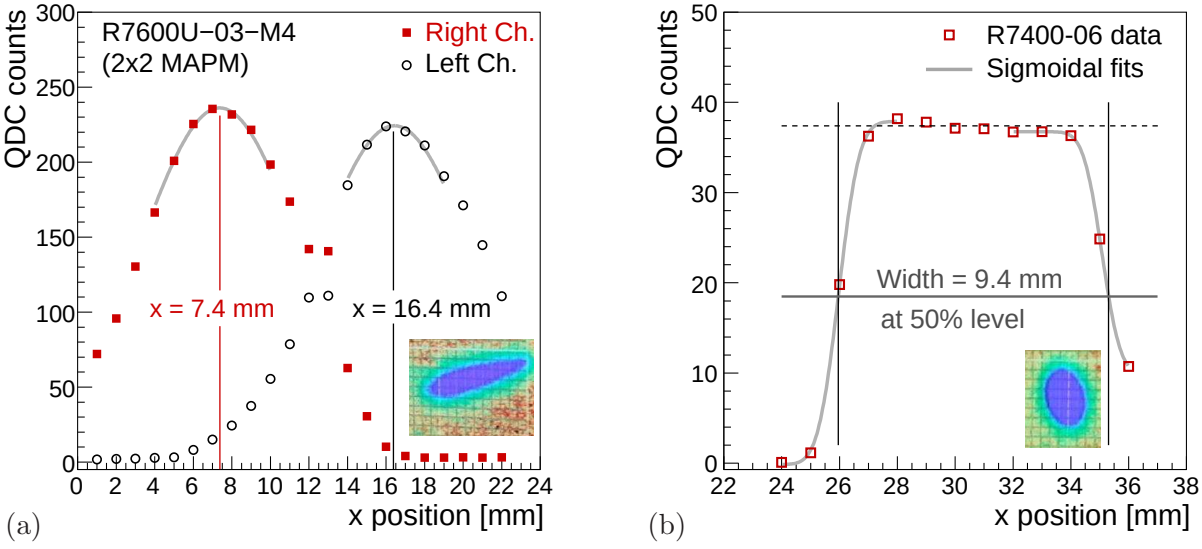

Figure 4: *Beam position scan data recorded with (a) the 2×2 MAPM (860 V) and elongated beam spot, (b) the R7400U-06 SAPM (300 V) and round beam spot. - only relative x-values are relevant -*

Some of the detector dimensions, such as the channel width or the distance between channel centers, can be extracted from beam data. A comparison of these derived values with the given prototype specifications can be used to disentangle different effects connected either to the detector itself, to its alignment w.r.t. the beam line, or exclusively to the beam. Figure 4(a) shows x-scan data recorded with the 2×2 MAPM (R7600U-03-M4) and an ellipsoidally elongated beam spot. Two Gaussian fits indicate the respective channel centres to be at $x_{\text{right}} = (7.4 \pm 0.1)$ mm and $x_{\text{left}} = (16.4 \pm 0.1)$ mm, leading to a distance of $\Delta x = (9.0 \pm 0.2)$ mm. This agrees well with the nominal distance of $\Delta x_{nom} = (8.5 + 0.3)$ mm given by the channel width plus the thickness of the inter-channel wall. Figure 4(b) shows x-scan for the R7400U-06 single-anode photomultiplier (SAPM), where a broad plateau is observed. The width of the signal region is determined from two sigmoidal fits to the edges of the plateau at 50% of its height. The width is $w = (9.4 \pm 0.3)$ mm with the error dominated by the table position accuracy. This value is larger than the nominal width ($w_{nom} = 8.5$ mm) hinting towards residual misalignment and a non-Gaussian beam profile. The dominant reason for the MAPM data not exhibiting an equally clear plateau is the different beam spots delivered by ELSA, aside from possible cross-talk in case of the MAPM and incomplete channel coverage of the SAPM.

The anode of the 8×8 MAPM (R7600-00-M64) is finely segmented with 16 anode pads covering one detector channel, thus offering spatial resolution within a single channel. Two QDC channels were broken leaving only six channels to realise the readout configuration illustrated in figure 5(a). The numbers indicate the QDC channel utilised to read out the sum signal of either four or eight MAPM anode pads. Figure 5(b) shows the result of an x-scan across both detector channels. As expected, the signals in QDC channels 2 and 3 are about twice as large as in the other channels due to the different grouping of anode pads. The asymmetric response reflects the beam position. For each QDC channel, the largest signal is observed when the beam

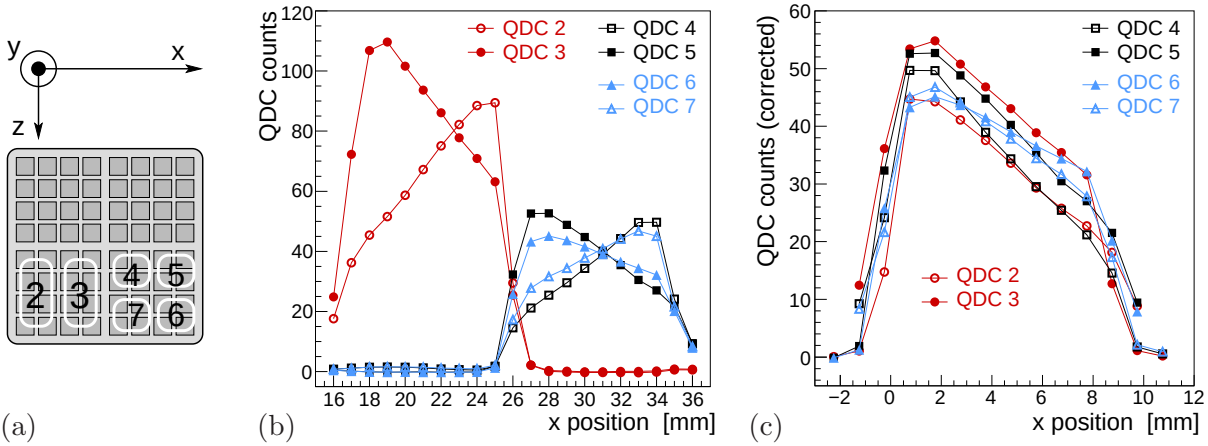

(a) (b) (c)

Figure 5: *Beam position scan data recorded with the 8×8 MAPM (500 V): (a) readout configuration, (b) x-scan across both channels, (c) same data, but with emphasis on shape and amplitude differences.*

enters on the opposite side of the detector channel confirming the prediction from simulation of one glancing angle reflection for most of the photons (see section 2). The same x-scan data is displayed again in figure 5(c), scaled and mirrored to correct for the different pad locations w.r.t. the beam position and the different number of pads grouped into one readout channel. Possible reasons for the remaining shape and amplitude differences comprise gain variations between the pads and residual detector misalignment.

From the beam position measurements with the 8×8 MAPM using QDC 4 to 7 on one detector channel, two different x- and z-asymmetries are determined according to the description at the end of section 2. They are displayed in Figure 6, together with those determined from simulated

data. The displayed errors correspond to 10% relative gain differences between the anode pads. Uncertainties in common between different pads cancel from the asymmetries.

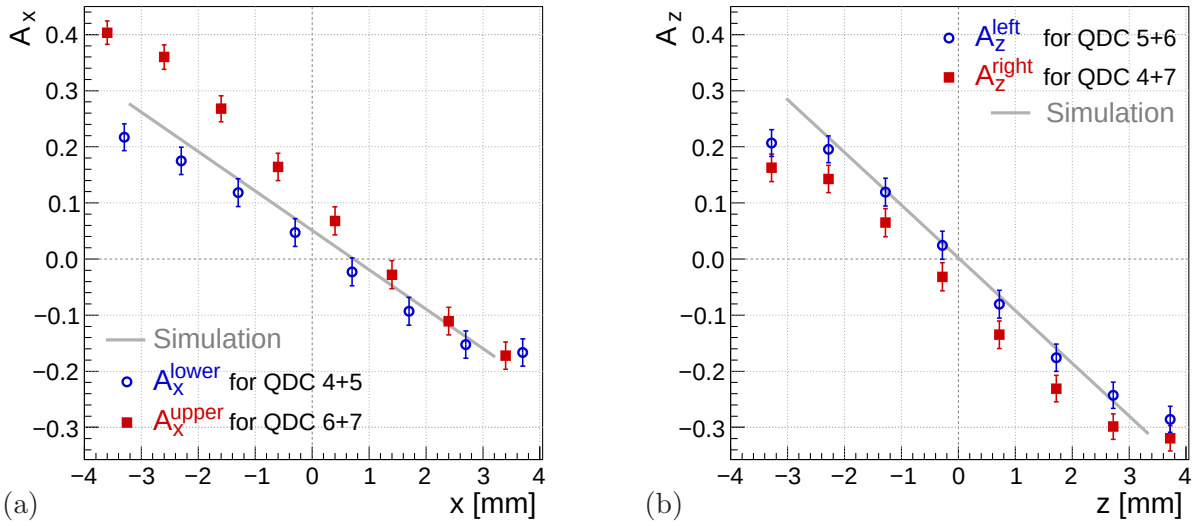

Figure 6: *Asymmetries A_x (a) and A_z (b) determined from position data recorded with the 8×8 MAPM. The error bars correspond to 10% relative gain variations between the anode pads, see figure 5(c).*

Qualitatively the measured asymmetries agree well with the simulation. A_x exhibits an offset in x and a more shallow slope as expected due to the lower reflectivity of the inter-channel wall, demonstrating the optical quality of the channel surfaces and a sufficiently detailed description in the simulation. Quantitatively, A_x^{upper} exhibits a different slope, while A_z^{right} is shifted suggesting residual misalignment and gain variations. These asymmetries can be exploited to determine the beam position even within a single detector channel, if a segmented photodetector is employed.

4. Conclusions

Compton polarimeters will be employed to measure the ILC beam polarisation to a precision of $\delta\mathcal{P}/\mathcal{P} = 0.25\%$ using Cherenkov detectors to register the scattered Compton electrons.

A compact two-channel prototype has been designed, simulated and constructed. It allows nearly all aspects of the final detector to be studied. The prototype has been operated successfully in a testbeam using four different PDs and the corresponding results are in good agreement with a detailed simulation. A newly developed method to extract intra-channel position information has been applied to the testbeam data in studying the detector response as a function of the beam position. This will lead to a determination of each channel's acceptance which is important to control systematic effects on the final polarisation measurements.

References

[1] ILC Global Design Effort and World Wide Study 2007 *ILC Reference Design Report - Vol. 2 and 3*
[2] Moortgat-Pick G A et al 2008 *Phys. Rept.* **460** 131-243 (*Preprint* hep-ph/0507011)
[3] Boogert S et al 2009 *JINST* **4** P10015 (*Preprint* 0904.0122v3 [physics.ins-det])
[4] GEANT4 Collaboration 2003 *Nucl. Instrum. Meth. Phys. Res.* A **506** 3 250-303
GEANT4 Collaboration 2006 *IEEE Trans. Nucl. Science* **53** 1 270-278
[5] Hamamatsu Photonics K.K. (datasheets)
R7600U-03-M4: `http://sales.hamamatsu.com/assets/pdf/parts_R/R5900U_R7600U_TPMH1291E03.pdf`
R7600-00-M64: `http://sales.hamamatsu.com/index.php?id=13195917`
R7400U-06: `http://sales.hamamatsu.com/assets/pdf/parts_R/R7400U_TPMH1204E07.pdf`
[6] Bartels C, Helebrant C, Käfer D and List J 2008 Nucl. Science Symp. IEEE (Dresden) Conf. Record 2313–14
[7] Helebrant C 2009 *Nucl. Instrum. Meth. Phys. Res.* A **610** 387-389

In search of new phenomena using polarisation – HERA and ILC (PhD thesis) Universität Hamburg, Germany
[8] Hillert W, 2006 *Eur. Phys. J.* A **28S1** 139